Journal of Materials Chemistry A

Pyrazine-incorporated graphdiyne nanofilm as a metal-free electrocatalyst for hydrogen evolution reaction

Journal:	*Journal of Materials Chemistry A*
Manuscript ID	TA-ART-07-2018-007347.R1
Article Type:	Paper
Date Submitted by the Author:	23-Aug-2018

Complete List of Authors:	Sakamoto, Ryota; The University of Tokyo, Department of Chemistry, Graduate School of Science Shiotsuki, Ryo; The University of Tokyo, Department of Chemistry, Graduate School of Science Wada, Keisuke; The University of Tokyo, Department of Chemistry, Graduate School of Science Fukui, Naoya; The University of Tokyo, Department of Chemistry, Graduate School of Science Maeda, Hiroaki; University of Tokyo, Department of Chemistry Komeda, Joe; The University of Tokyo, Department of Chemistry, Graduate School of Science Sekine, Ryosuke; The University of Tokyo, Department of Chemistry, Graduate School of Science Harano, Koji; The University of Tokyo, Nishihara, Hiroshi; University of Tokyo, Department of Chemistry

Journal Name

ARTICLE

Pyrazine-incorporated graphdiyne nanofilm as a metal-free electrocatalyst for hydrogen evolution reaction

Received 00th January 20xx,
Accepted 00th January 20xx

DOI: 10.1039/x0xx00000x

www.rsc.org/

Ryota Sakamoto,*[a,b] Ryo Shiotsuki,[a] Keisuke Wada,[a] Naoya Fukui,[a] Hiroaki Maeda,[a] Joe Komeda,[a] Ryosuke Sekine,[a] Koji Harano,[a] and Hiroshi Nishihara[a]

A graphdiyne (**GDY**) analogue that features pyrazine as the aromatic core (**PR-GDY**) was synthesized under air using a liquid/liquid interfacial synthesis. Optical microscopy, SEM, and AFM revealed the sheet morphology of **PR-GDY** with a typical thickness of 20 nm in AFM, while TEM disclosed its amorphous nature. It served as a metal-free electrocalatyst for the hydrogen evolution reaction (HER) from water. The presence and presence of the butadiynyl linker and terminal ethynyl group, respectively, was confirmed by Raman spectroscopy. Polymerization to **PR-GDY** afforded optical bandgap narrowing compared with the corresponding monomer. XPS provided a ratio of 2:1 for the sp and sp^2 carbons. Moreover, a single gaussian was fitted with the N 1s peak, ascribable to the pyridinic nitrogen. Such selective doping of heteroatoms as for the chemical environment is hard to realize in carbon materials. **PR-GDY** was subjected to TGA, such that its thermal stability up to 300°C was confirmed. N_2 adsorption-desorption isotherms featured a typical type I adsorption behavior with micropores, with Brunauer–Emmett–Teller surface area and mean pore size of, respectively, 408 m^2g^{-1} and 0.8 nm. A series of electrochemical measurements was conducted to evaluate the HER activity of **PR-GDY**. The HER performance of **GDY** was only slightly better than glassy carbon, while that of **PR-GDY** was improved significantly in both acidic and basic aqueous media with an onset potential of -275 mV (vs reversible hydrogen electrode, RHE), and -475 mV to achieve a current density of 10 mA cm^{-2} in 0.5 M H_2SO_4, and –270 and –710 mV in (0.1M $NaHCO_3$ + 0.1M Na_2CO_3). The present work demonstrates experimentally that **PR-GDY** serves as a metal-free HER electrocatalyst, and manifestly that pyridinic nitrogen enhances the electrocatalytic activity in carbon materials.

Introduction

Graphdiyne (**GDY**) as an allotrope of elemental carbon has collected recent attention of chemists.[1] Its π-conjugated 2D hexagonal lattice is reminiscent of graphene, though **GDY** features the coexistence of sp- and sp^2- carbons, which makes **GDY** different from graphene sufficiently. In 2010, Li and coworkers reported the bulk synthesis of **GDY** using hexaethynylbenzene as a monomer,[2] and modifications of the synthetic procedure produced **GDY** nanowalls and nanofilms.[3,4] A wide variety of applications for **GDY**, such as lithium ion battery and solar cells, was also reported by Li and coworkers.[5] On the other hand, our group demonstrated liquid/liquid and gas/liquid interfacial syntheses for **GDY**.[6] Of note is the latter process allowed us to create **GDY** nanosheets of better quality with regular hexagonal domains. One of the next directions for the **GDY** research is to expand the variation, as the starting

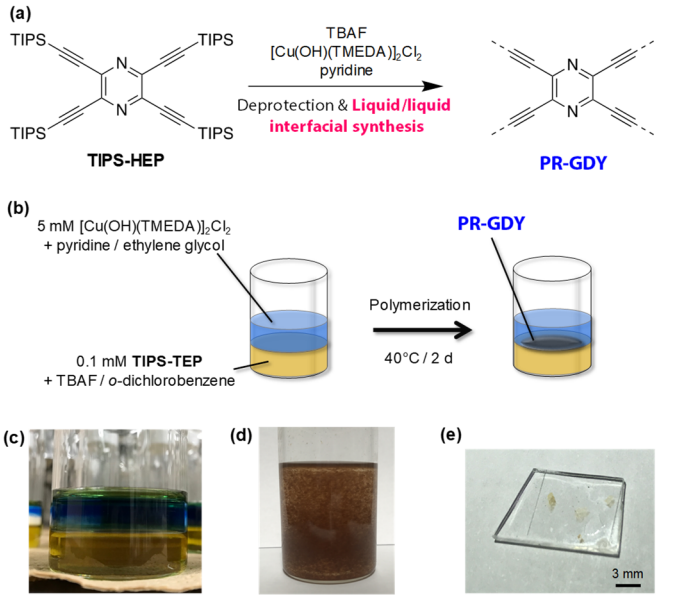

Fig. 1 (a) Synthetic scheme for **PR-GDY**. (b) Schematic illustration of liquid/liquid interfacial synthesis for **PR-GDY**. (c) Photograph of the liquid/liquid interfacial synthesis. (d) **PR-GDY** suspended in acetone. (e) Photograph of a **PR-GDY** film transferred on quartz.

[a] *Graduate School of Science, The University of Tokyo, 7-3-1, Hongo, Bunkyo-ku, Tokyo 113-0033, Japan.*
[b] *JST-PRESTO, 4-1-8, Honcho, Kawaguchi, Saitama 332-0012, Japan*

† Footnotes relating to the title and/or authors should appear here.
Electronic Supplementary Information (ESI) available: SEM/EDX for **PR-GDY**, two possible 2D lattices for **PR-GDY**, optical bandgap determination for **PR-GDY**, quantification of the C/N ratio of **PR-GDY** in XPS, gas adsorption isotherms and pore size analysis for **PR-GDY**, EIS and its equivalent circuit analysis for **PR-GDY**, durability against HER for **PR-GDY**. See DOI: 10.1039/x0xx00000x

monomer can be tuned diversely. In this context, several **GDY** analogues have been published recently.[7-10] In this communication, a pyrazine-cored **GDY** analogue, **PR-GDY**[11] (Fig. 1a), is reported to demonstrate its metal-free electrochemical catalytic activity for the hydrogen evolution reaction (HER[12]). HER may be regarded as one of the most fundamental but important reaction steps in electrochemical water splitting. From the viewpoint of application, HER is expected to play a vital role in the hydrogen economy, converting electricity into hydrogen as chemical energy and fuel. In this context, metal-free HER catalyst is being sought urgently for sustainability. There are several reports on the HER activity of the **GDY** family, though, all of them were conjugated with metal components such as MoS_2 and Co nanoparticles.[13] One of the chief strategies to realize metal-free electrocatalysts is incorporation of heteroatoms into carbon materials.[14] However, high-temperature syntheses or post-synthetic modifications for heteroatom-doped carbon materials often induce heterogeneous chemical environments for the dopants (e.g. pyridinic, pyrrolic, quaternary, and graphitic nitrogens). This often humpers the understanding of the heteroatom effect on the electrocatalysis. In sharp contrast, **GDY** belongs to covalent organic frameworks (COFs) or molecule-based nanosheets, where the chemical structures of the monomer units are more or less preserved.[15] In the case of **PR-GDY**, pyridinic N should be incorporated exclusively as a nitrogen composition. This provides us with simple discussion on the effect of the pyridinic nitrogen on HER.

Synthesis

PR-GDY was synthesized by liquid/liquid interfacial synthesis (Fig. 1b,c).[6,16] *o*-Dichlorobenzene as the bottom layer contained 0.2 mM triisopropylsilyl-protected tetraethynylpyrazine (**TIPS-TEP**), while the top layer comprised ethylene glycol with 5 mM di-μ-hydroxy-bis(*N*,*N*,*N*',*N*'-tetramethylenediamine) copper(II) ([Cu(OH)TMEDA]$_2$Cl$_2$) as a catalyst for oxidative alkyne dimerization. The TIPS protecting group was then removed in situ using tetrabutylammonium fluoride (TBAF), and the bilayer system was kept undisturbed for 2 d at 40°C to obtain **PR-GDY** as a brown film showing up at the interface. Note that previous synthesis for **GDY** often require inert atmospheres, but the present synthetic process may be conducted under air. This point is beneficial for mass production and potential materials application. The resultant brown film was insoluble in any solvent and upon sonication (Fig. 1d), reflecting its polymeric nature. The brown color was confirmed in a photograph of **PR-GDY** on a quartz substrate (Fig. 1e). A typical lateral size of **PR-GDY** after the washing and sonication process was 0.5-1.0 mm. The significant bathochromic color change in **PR-GDY** (pale-yellow for TIPS-TEP) should reflect its π-conjugated electronic structure (vide infra).

Microscopic analysis

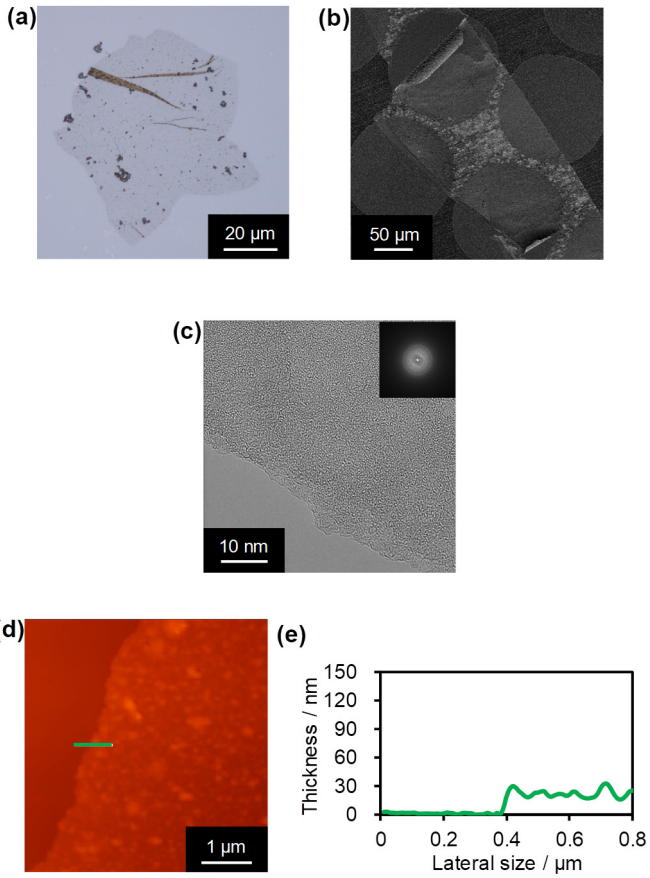

Fig. 2 (a-d) A series of micrographs for **PR-GDY** nanofilms. (a) Optical micrographs on a SiO_2/Si substrate. (b) SEM image (acceleration voltage: 1 kV) on a copper TEM grid covered with a microgrid. (c) Bright-field TEM image (acceleration voltage: 80 kV) on the grid with a FFT pattern as an inset. (d) AFM height image on a SiO_2/Si substrate. (e) Cross-section analysis along the blue line in (d).

The **PR-GDY** nanofilm may be transferred onto various substrates and TEM grids, which was subjected to various microscopic analyses. Fig. 2 assembles a series of microscopic images for **PR-GDY** nanofilms. Optical microscopy revealed a sheet structure with a flat and smooth texture, and small folded parts (Fig. 2a). Similarly, the SEM image disclosed a submillimeter-sized sheet framework (Fig. 2b). In addition, EDS accompanying SEM envisioned constitutive C and N elements, while Cu and Cl derived from the catalyst for the polymerization were absent (Fig. S1). On the other hand, the bright-field TEM image did not show any periodic structures, suggesting an amorphous nature of the **PR-GDY** nanofilm (Fig. 2c). The amorphicity is presumably induced by the two possible 2D frameworks (Fig. S2), which makes it arduous to form 2D periodicity. A typical thickness of the **PR-GDY** nanofilm was determined to be ca. 20 nm in AFM (Fig. 2d,e).

Spectroscopic analysis

PR-GDY was also characterized by Raman spectroscopy (Fig. 3a) and X-ray photoelectron spectroscopy (XPS, Fig. 3b-d). In the Raman spectrum a characteristic butadiynyl band was observed

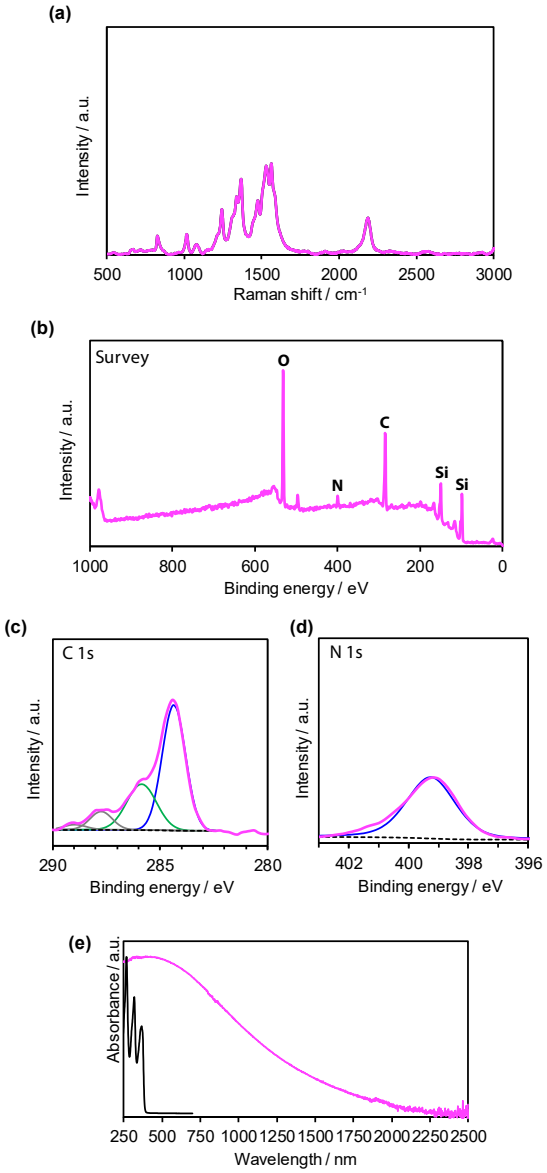

Fig. 3 (a) Raman spectrum for **PR-GDY** on Au-coated mica. (b) XPS survey scan for **PR-GDY** on SiO_2/Si. (c) C 1s narrow scan (magenta) for **PR-GDY** with decovoluted peaks assignable to sp^2 (blue), sp (green), oxygenized carbon species (gray), and background (black dashed). (d) N 1s narrow scan (magenta) for **PR-GDY** with decovoluted peaks assignable to pyridinic nitrogen (blue) and background (black dashed). (e) Normalized absorption spectra of **PR-GDY** (magenta) and **TIPS-TEP** (black).

at 2183 cm^{-1}, but that form terminal alkyne at around 2100-2120 cm^{-1} was absent. XPS survey scan verified the existence of nitrogen and carbon, as well as the absence of copper 2p bands (ca. ~930 eV) and chlorine 2p bands (ca. ~200 eV) stemming from $[Cu(OH)TMEDA]_2Cl_2$ catalyst. The XPS narrow-scan peak for C 1s (Fig. 3c) was deconvoluted into four Gaussians: the major contributions are derived from constitutive sp and sp^2 carbons with a ratio of 2:1, being consistent with the chemical composition. On the other hand, the minor contributions at higher binding energies originate from oxygenated carbon species, with an oxygen/carbon ratio of 0.2. On the other hand, the N 1s peak may be fitted with a single Gaussian at 399.2 eV, ascribable to the pyridinic nitrogen derived from **TIPS-TEP**

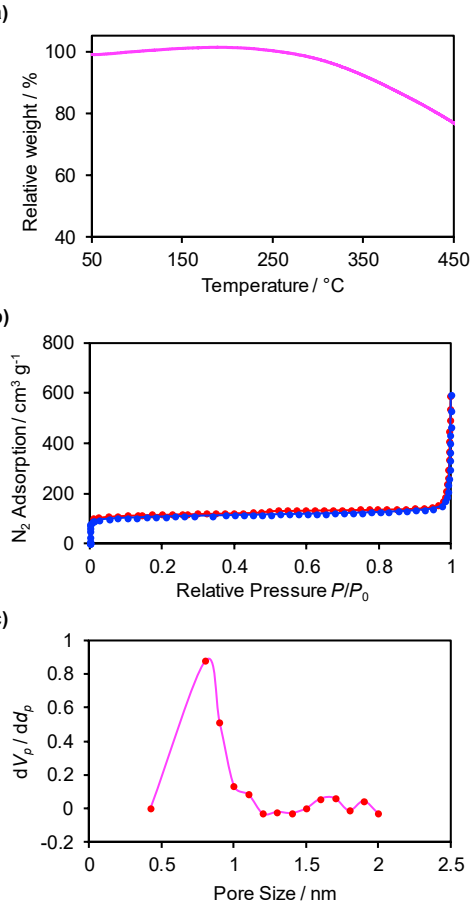

Fig. 4 (a) TGA for **PR-GDY** under a nitrogen atmosphere. (b) N_2 adsorption (blue symbols) and desorption (red symbols) isotherms at 77 K for **PR-GDY**. (c) Poresize distribution analyzed by the MP method for the N_2 isotherm.

monomer.[17] This indicative selective nitrogen doping was attained in **PR-GDY**, which is hardly realizable in general carbon materials. The C/N ratio of **PR-GDY** was determined to be 6.1, consistent with the ideal value of 6 (Fig. S3). Fig. 3e represents normalized absorption spectra of **TIPS-TEP** monomer and **PR-GDY**. The former possessed an optical gap of 3.20 eV. In sharp contrast, the latter underwent a significant redshift and broadening in comparison with the former: its optical bandgap was determined to be ~0.55 eV (Fig. S4). This series of experimental facts is indicative of the highly developed π-conjugated polymeric structure of **PR-GDY**.

Thermogravimetric and porosity analysis

Thermogravimetric analysis (TGA) indicated that **PR-GDY** possessed good thermal durability up to ca. 300°C (Fig. 4a), which was tolerable for polymer materials. The existence of micropores in **PR-GDY** was confirmed by measuring N_2 and H_2O adsorption and desorption isotherms (Fig. 4b and S5). The N_2 adsorption and desorption isotherms exhibited a typical type I adsorption behavior with micropores, with a Brunauer–Emmett–Teller (BET) surface area of 408 m^2g^{-1}. The main pore size was determined to be 0.8 nm (Fig. 4c).

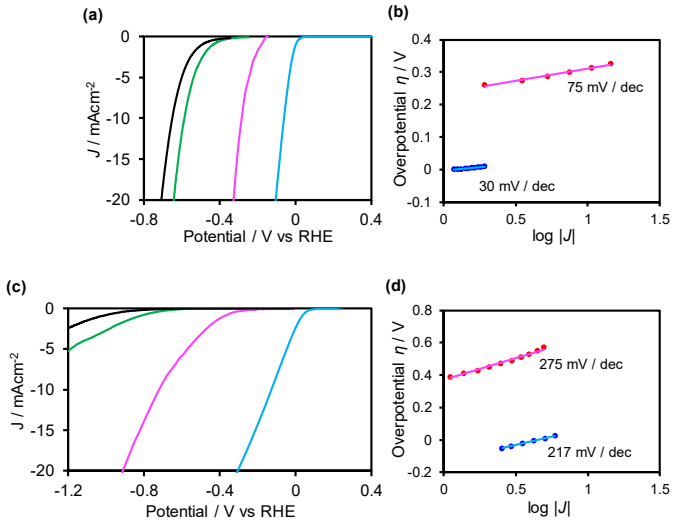

Fig. 5 (a,c) Linear sweep voltammograms for bare GC (black solid), GC modified with **PR-GDY** (magenta), GC modified **GDY** (green), and Pt (blue) in aqueous 0.5M H_2SO_4 and 0.1M $NaHCO_3$ + 0.1M Na_2CO_3, respectively. (b,d) Tafel plots for GC modified with **PR-GDY** and Pt in aqueous 0.5M H_2SO_4 and 0.1M $NaHCO_3$ + 0.1M Na_2CO_3, respectively.

HER activity

The HER activity was investigated through a series of electrochemical measurements (Fig. 5, S5, S6). Linear sweep voltammetry (LSV) was conducted using a typical three-electrode setup in aqueous 0.5M H_2SO_4 (Fig. 5a), where glassy carbon (GC) decorated with **PR-GDY** was employed as a working electrode. The modification of the GC electrode was performed by depositing a **PR-GDY** suspension in *N*-methylpyrrolidone with the aid of carbon black and polyvinylidene difluoride (PVDF). For comparison, plain **GDY**, bare GC, and Pt electrodes were also subjected to LSV, the results of which were overlaid on the LSV for **PR-GDY**. GC underwent poor hydrogen evolution even under large overpotentials. Similarly, **GDY** did not exhibited an outstanding HER performance, with an onset potential of -470 mV, and –590 mV to achieve a HER current density of 10 mA cm^{-2}. In contrast, **PR-GDY** on GC much better HER activity than plain **GDY** and bare GC; **PR-GDY** featured an onset potential of –275 mV, and a current density of 10 mA cm^{-2} was attained at an electrode potential of –475 mV. Tafel plot for **PR-GDY** on GC is shown in Fig. 5b, disclosing relatively a small slope of 75 mV/dec, indicating that **PR-GDY** facilitates the HER reaction.[18] Electrochemical impedance spectroscopy (EIS) provided us with Nyquist plots that may be reproduced using a typical equivalent circuit that included charge-transfer and internal resistances, and a capacitor-like fragment (Fig. S6). The HER performance was also verified in a basic aqueous medium (0.1M $NaHCO_3$ + 0.1M Na_2CO_3), again highlighting good HER activity for **PR-GDY** (–270 and –710 mV for onset and 10 mA cm^{-2} potentials) on GC over plain **GDY** (–600 and –1410 mV; Fig. 5c,d). Acceptable durability for **PR-GDY** was confirmed in 0.5M H_2SO_4 and 0.1M $NaHCO_3$ + 0.1M Na_2CO_3 after 1000 cycles (Fig. S7). Together with the selective elemental doping process in **GDY** analogues, this series of electrochemical results indicates manifestly that the pyridinic nitrogen in **PR-GDY** enhances the HER activity.

Conclusions

Pyrazine-cored GDY analogue **PR-GDY** was synthesized by means of liquid/liquid interfacial reaction under air. A series of microscopic analyses disclosed the nanofilm morphology of **PR-GDY** with a thickness of ca. 20 nm. Raman spectroscopy indicated the existence and absence of the butadiyne linker and terminal alkyne group, respectively, while wide-scan XPS and SEM/EDS detected the constitutive elements but no Cu residue used as the alkyne-alkyne dimerization catalyst. Narrow-scan XPS provided information on the chemical environments of carbon (sp : sp^2 = 2 : 1), and nitrogen (solely pyridinic). UV/vis spectroscopy found a substantially narrowed optical bandgap in **PR-GDY** upon polymerization. TGA disclosed the thermal stability of **PR-GDY** up to 300°C. Gas adsorption and desorption isotherms disclosed a typical type I adsorption behavior with micropores (BET surface area and chief pore size of 408 m^2g^{-1} and 0.8 nm). **PR-GDY** served as a metal-free electrode catalyst for HER in both acidic and basic aqueous solutions, which was investigated by LSV, Tafel plot, and EIS. **PR-GDY** featured onset potential and potential to achieve a current density of 10 mA cm^{-2} of –275 and –475 mV vs RHE in 0.5 M H_2SO_4, while they were –270 and –710 mV in 0.1M $NaHCO_3$ + 0.1M Na_2CO_3. These potential values were much better than plain **GDY**, indicating manifestly that the pyridinic nitrogen reinforced the HER activity of **PR-GDY**. Such experimental study is hardly realizable in carbon materials where selective and quantitative elemental doping is a tough task, thereby allowing the **GDY** family to be a distinctive nanocarbons. This work has expanded the futurity of the **GDY** family as functional 2D nanomaterials.

Experimental

Materials

All chemicals were purchased from Tokyo Chemical Industry Co., Ltd., Kanto Chemical Co., or Wako Pure Chemical Industries, Ltd., unless otherwise stated. They were used without further purification. Water was purified using a Milli-Q purification system (Merck KGaA). A Si(100) wafer covered with an 85 nm SiO_2 layer was purchased from Electronics and Materials Corp., Ltd, and hydrophobized using HMDS as follows. The Si substrate was placed into a desiccator with HMDS (0.1 mL). The desiccator was then purged with argon and left to stand overnight. The hydrophobized substrate was dried in vacuo overnight and stored under argon. A TEM grid with a holey carbon matrix (NS-C15) was purchased from Okenshoji Co., Ltd. Tetrakis[(triisopropylsilyl)ethynyl]pyrazine (**TIPS-TEP**), and di-μ-hydroxy-bis(*N*,*N*,*N*',*N*'-tetramethylenediamine) copper(II) ($[Cu(OH)TMEDA]_2Cl_2$) were synthesized according to the literature.[19] **GDY** for the HER activity evaluation was prepared using a liquid/liquid interfacial reaction described in our previous report.[6]

Instruments

Optical microscopic images were taken using an optical microscope (LV100, Nikon) equipped with a camera (DP71, Olympus). SEM/EDS data were collected using a JEOL JSM-7400FNT equipped with an EDS analyzer (JEOL EX-2300) with an acceleration voltage of 10 kV and an FEI Magellan 400L instrument with an acceleration voltage of 1 kV. TEM observations were carried out on a JEOL JEM-ARM200F instrument equipped with an aberration corrector and cold field emission gun (point resolution: 0.10 nm) at acceleration voltages of E = 80 kV, under 1×10^{-5} Pa in the specimen column and with typical spherical aberration values of 1–3 μm. The imaging instrument was a CMOS camera (Gatan OneView, 4,096 × 4,096 pixels) and operated in binning 2 mode (output image size: 2,048 × 2,048 pixels). XPS data were acquired using an ULVAC-PHI 5000 VersaProbe spectrometer. Al Kα (15 kV, 25 W) radiation was used as the X-ray source, and the beam was focused on a 100 μm^2 area. The spectra were analyzed using MultiPak Software and standardized using the Si 2p peak originating from SiO_2 at 103.3 eV. Raman spectra were collected using a HORIBA LabRAM HR Evolution (laser wavelength is 633 nm). AFM measurements were carried out using a BRUKER Multimode-8HR-AM-SR under ambient conditions in the ScanAsyst mode with a silicon cantilever. UV-vis-NIR absorption spectra were recorded with JASCO V-570 equipped with an integrating sphere photometer (ISN-470). TGA was performed under nitrogen atmosphere by Rigaku Thermo Plus2 TG8120 instrument. Al_2O_3 was used as a reference compound, and both **PR-GDY** and Al_2O_3 were mounted on Al pans. The temperature was controlled from room temperature to 500°C at a scan rate of 10°C s^{-1}.

Liquid/liquid interfacial synthesis of PR-GDY

Under an ambient atmosphere, to a solution of Tetrakis[(triisopropylsilyl)ethynyl]pyrazine (**TIPS-TEP**; 1.6 mg, 2.0 μmol) in 10 mL of *o*-dichlorobenzene, tetrabutylammonium fluoride (1 M in 10 μL of THF, 10 μmol) was added. Then, the solution was poured into a glass cylinder with a diameter of 35 mm. $[Cu(OH)(TMEDA)_2]Cl_2$ (5 mM) and pyridine (10 mM) in 10 mL of ethylene glycol was added gently added onto the organic phase. The reaction system was aged for 48 hours at 40 °C and brown film of **PR-GDY** was elucidated at the interface. The **PR-GDY** nanofilm was collected and washed with acetone, aqueous HCl (1 M), aqueous NH_3 and pure water.

Electrochemical analysis

Electrochemical experiments were carried out using an electrochemical analyzer (650DT, ALS). The decoration of a GC electrode with **PR-GDY** was conducted as follows. **PR-GDY** (0.9 mg) and carbon black (1.0 mg) were added to the 16.6 mg of polyvinylidene difluoride (PVDF) solution in NMP (12%w/w) and sonicated for 10 min. The resultant suspension was grinded in the mortar to be homogenized. 0.6 mg of the sample was placed on a 5mmϕ GC electrode surface and heated at 40°C under an ambient condition to use for the HER measurement. This modified GC electrode was used as a working electrodes in a three-electrode electrochemical cell holding a Pt wire as a counter electrode, and the Ag/AgCl redox couple in saturated KClaq as a reference electrode. Bare GC or Pt was also used as a working electrode as references. The observed working electrode potential (E_{obs}) was converted to the potential versus RHE (E) using eq. (1)

$$E = E_{obs} + 0.199 + 0.059\ pH \quad (1)$$

The electrolyte solution was deoxygenated with pure Ar prior to the measurement. LSV was conducted at a sweep rate of 20 mV s^{-1}.

Conflicts of interest

There are no conflicts to declare.

Acknowledgements

The present work was chiefly supported by JST-PRESTO "Hyper-nano-space design toward Innovative Functionality" to R.Sakamoto (JPMJCR15F2). The authors also acknowledge Grants-in-Aid from MEXT of Japan (Nos. 26708005, 26220801, 16H00900, 17H03028, 17H05354, 17H05355, areas 2506 [Science of Atomic Layers] and 2802 [Coordination Asymmetry]) and Japan Agency for Science and Technology (CREST; JPMJCR14L4 and JPMJCR15F2). R.S. is grateful to Iketani Science and Technology Foundation, Kumagai Foundation for Science and Technology, Foundation for Interaction in Science & Technology, The Foundation for The Promotion of Ion Engineering, Foundation Advanced Technology Institute, Izumi Science and Technology Foundation, LIXIL JS Foundation, Tonen General Sekiyu R&D Encouragement and Assistance Foundation, The Iwatani Naoji foundation, Hitachi Metals · Materials Science Foundation, The Murata Science Foundation, Kato foundation for Promotion of Science, and Yashima Environment Technology Foundation for financial supports.

Notes and references

1 Z. Jia, Y. Li, Z. Zuo, H. Liu, C. Huang, Y. Li, *Acc. Chem. Res.*, 2017, **50**, 2470.
2 G. Li, Y. Li, H. Liu, Y. Guo, Y. Li, D. Zhu, *Chem. Commun.*, 2010, **46**, 3256.
3 J. Zhou, X. Gao, R. Liu, Z. Xie, J. Yang, S. Zhang, G. Zhang, H. Liu, Y. Li, J. Zhang, Z. Liu, *J. Am. Chem. Soc.*, 2015, **137**, 7596.
4 X. Qian, H. Liu, C. Huang, S. Chen, L. Zhang, Y. Li, J. Wang, Y. Li, *Sci. Rep.*, 2015, **5**, 7756.
5 (a) H. Shang, Z. Zuo, H. Zheng, K. Li, Z. Tu, Y. Yi, H. Liu, Y. Li, Y. Li, *Nano Energy*, 2018, **44**, 144. (b) J. Xiao, J. Shi, H. Liu, Y. Xu, S. Lv, Y. Luo, D. Li, Q. Meng, Y. Li, *Adv. Energy Mater.*, 2015, **5**, 1401943.
6 R. Matsuoka, R. Sakamoto, K. Hoshiko, S. Sasaki, H. Masunaga, K. Nagashio, H. Nishihara, *J. Am. Chem. Soc.*, 2017, **139**, 3145.
7 J. He, N. Wang, Z. Cui, H. Du, L. Fu, C. Huang, Z. Yang, X. Shen, Y. Yi, Z. Tu, Y. Li, *Nat. Commun.*, 2017, **8**, 1172.
8 P. Prabakaran, S. Satapathy, E. Prasad, S. Sankararaman, *J. Mater. Chem. C*, 2018, **6**, 380.

9 H. Shang, Z. Zuo, H. Zheng, K. Li, Z. Tu, Y. Yi, H. Liu, Y. Li, Y. Li, *Nano Energy*, 2018, **44**, 144.
10 R. Matsuoka, R. Toyoda, R. Shiotsuki, N. Fukui, K. Wada, H. Maeda, R. Sakamoto, S. Sasaki, H. Masunaga, K. Nagashio, H. Nishihara, *ACS Appl. Mater. Interfaces*, 2018, doi:10.1021/acsami.8b00743
11 The synthesis of **PR-GDY** was first reported in X. Kan, Y. Ban, C. Wu, Q. Pan, H. Liu, J. Song, Z. Zuo, Z. Li, Y. Zhao, *ACS Appl. Mater. Interfaces*, doi:10.1021/acsami.7b17326. Its functionality was not reported therein.
12 a) J.-X. Feng, H. Xu, Y.-T. Dong, X.-F. Lu, Y.-X. Tong, G.-R. Li, *Angew. Chem.Int. Ed.* 2017, **56**,2960; b) J.-X. Feng, J.-Q. Wu, Y.-X. Tong, G.-R. Li, *J. Am. Chem. Soc.*, 2018, **140**, 610; c) L.-J. Chen, S. Chen, Y. Qin, L. Xu, G.-Q. Yin, J.-L. Zhu, F.-F. Zhu, W. Zheng, X. Li, H.-B. Yang, *J. Am. Chem. Soc.*, 2018, **140**, 5049.
13 a) L. Hui, D. Jia, H. Yu, Y. Xue, Y. Li, *ACS Appl. Mater. Interfaces* doi: 10.1021/acsami.8b01887; b) H. Yu, Y. Xu, L. Hui, C. Zhang, Y. Zhao, Z. Li, Y. Li, *Adv. Funct. Mater.*, 2018, **28**, 1707564; c) Y. Yao, Z. Jin, Y. Chen, Z. Gao, J. Yan, H. Liu, J. Wang, Y. Li, S. Liu, *Carbon*, 2018, **129**, 228; d) Y. Xue, Z. Zuo, Y. Li, H. Liu, Y. Li, *Small*, 2017, **13**, 1700936; e) J. Li, J. Li, X. Zhou, Z. Xia, W. Gao, Y. Ma, Y. Qu, *ACS Appl. Mater. Interfaces*, 2016, **8**, 31083; f) Y. Xue, Y. Guo, Y. Yi, Y. Li, H. Liu, D. Li, W. Yang, Y. Li, *Nano Energy*, 2016, **30**, 858.
14 a) Y. Zheng, Y. Jiao, Y. Zhu, L. H. Li, Y. Han, Y. Chen, A. Du, M. Jaroniec, S. Z. Qiao, *Nat. Communm.*, 2014, **5**, 3783; b) Z. Yong, N. Ryuhei, K. Kazuhide, N. Shuji, H. Kazuhito, *Nat. Commun.*, 2013, **4**, 2390; c) J.-X. Feng, H. Xu, S.-H. Ye, G. Ouyang, Y.-X. Tong, G.-R. Li, *Angew. Chem. Int. Ed.*, 2018, **56**, 8120.
15 a) P. Payamyar, B. T. King, H. C. Öttinger, A. D. Schlüter, *Chem. Commun.*, 2016, **52**, 18; b) D. Rodríguez-San-Miguel, P. Amo-Ochoa, F. Zamora, *Chem. Commun.*, 2016, **52**, 4113; c) R. Sakamoto, K. Takada, T. Pal, H. Maeda, T. Kambe, H. Nishihara, *Chem. Commun.*, 2017, **53**, 5781; d) S. N. Talapaneni, J. Kim, S. H. Je, O. Buyukcakir, J. Oh, A. Coskun, *J. Mater. Chem. A*, 2017, **5**, 12080.
16 a) T. Kambe, R. Sakamoto, K. Hoshiko, K. Takada, J.-H. Ryu, S. Sasaki, J. Kim, K. Nakazato, M. Takata and H. Nishihara, *J. Am. Chem. Soc.*, 2013, **135**, 2462; b) T. Kambe, R. Sakamoto, T. Kusamoto, T. Pal, N. Fukui, T. Shimojima, Z. Wang, T. Hirahara, K. Ishizaka, S. Hasegawa, F. Liu and H. Nishihara, *J. Am. Chem. Soc.*, 2014, **136**, 14357; c) R. Sakamoto, K. Hoshiko, Q. Liu, T. Yagi, T. Nagayama, S. Kusaka, M. Tsuchiya, Y. Kitagawa, W.-Y. Wong, H. Nishihara, *Nat. Commun.*, 2015, **6**, 6713; d) R. Sakamoto, T. Yagi, K. Hoshiko, S. Kusaka, R. Matsuoka, H. Maeda, Z. Liu, Q. Liu, W.-Y. Wong and H. Nishihara, *Angew. Chem. Int. Ed.*, 2017, **56**, 3526; e) K. Takada, R. Sakamoto, S.-T. Yi, S. Katagiri, T. Kambe and H. Nishihara, *J. Am. Chem. Soc.*, 2015, **137**, 4681; f) T. Tsukamoto, et al. *J. Am. Chem. Soc.*, 2017, **139**, 5359.
17 R. Walczak, B. Kurpil, A. Savateev, T. Heil, J. Schmidt, Q. Qin, M. Antonietti, M. Oschatz, Angew. Chem. Int. Ed. doi: 10.1002/anie.201804359
18 J. Duan, S. Chen, B. A. Chambers, G. G. Andersson, S. Z. Qiao, *Adv. Mater.*, 2015, **27**, 4234.
19 a) A. Petrosyan, P. Ehlers, A.-E. Surkus, T. V. Ghochikyan, A. S. Saghyan, S. Lochbrunnere, P. Langer, *Org. Biomol. Chem.,* 2016, **14**, 1442; b) J. P. Collman, M. Zhong, C. Zhang, S. Costanzo, *J. Org. Chem.*, 2001, **66**, 7892.

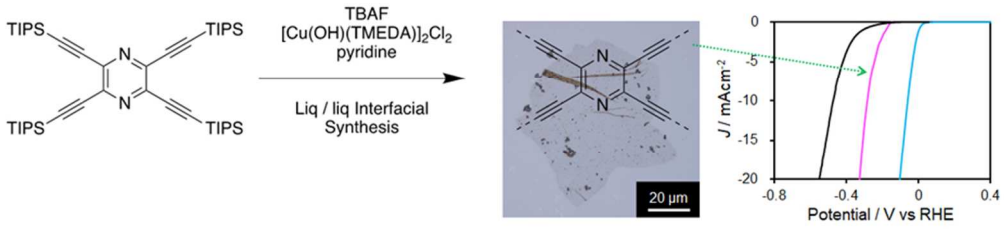

78x17mm (300 x 300 DPI)

A graphdiyne (GDY) analogue that features pyrazine as the aromatic component was synthesized under air using a liquid/liquid interfacial synthesis. It served as a metal-free electrocalatyst for the hydrogen evolution reaction (HER) from water.